

# Performance Study of A Near-Optimum Modulation Diversity Assisted Ultra-Wideband Receiver

Jin Tang, Zhengyuan Xu  
Department of Electrical Engineering  
University of California  
Riverside, CA 92521  
{jintang,dxu}@ee.ucr.edu

**Abstract**—A novel modulation diversity assisted (MDA) ultra-wideband (UWB) communication system was recently proposed. In this scheme, pulse position modulation and pulse amplitude modulation are applied to successive transmitted pulses alternately. The resulting modulation diversity helps to overcome channel estimation difficulties in typical UWB channels and permits low complexity receiver design. This paper considers a near-optimum receiver for MDA-UWB systems and studies its performance. A maximum likelihood (ML) estimator is also derived as a performance benchmark. Although the proposed receiver has a very simple structure, its performance approaches that of the ML receiver as signal-to-noise ratio increases. Our theoretical analysis is verified by computer simulations.

## I. INTRODUCTION

A transmitted reference (TR) scheme has gained renewed interests in the ultra-wideband (UWB) community because it bypasses the difficulty of channel estimation and has a low complexity receiver structure[1], [2]. Such a system transmits a pulse pair for each data symbol. A pulse without data modulation is transmitted before each data-modulated pulse. Because the two pulses undergo the same multipath channel, the first pulse in the doublet can be used as a reference to detect the information carried on the second pulse. Such a simple TR transceiver avoids explicit estimation of a possibly long UWB channel while still being capable of capturing full multipath energy. However, a TR system is bandwidth inefficient and power inefficient by transmitting information-free reference pulses. Consequently, many works are contributed to address these issues. For example, [3] and [4] reduce the separation between reference and data pulses to improve bandwidth efficiency. In [5] and [6], a QPSK-TR modulation scheme and a pulse interval amplitude modulation (PIAM) scheme are presented respectively to transmit two data bits in one doublet. [7] proposes a pilot waveform assisted modulation scheme to reduce the number of reference pulses and discusses power allocation between the pilot and data.

Recently, we developed a new modulation diversity assisted (MDA) UWB system [8], [9]. At the transmitter side, pulse

position modulation (PPM) and pulse amplitude modulation (PAM) are employed to a pulse train in an alternating way. As a result, two neighboring pulses have different modulation formats. Because information is modulated differently on pulses, diversity is created. At the receiver end, diversity can be utilized to assist template estimation and symbol detection. Although there are some connections between the MDA and TR transmission schemes, it can be shown the MDA scheme can improve both the bandwidth efficiency and energy efficiency over the TR scheme. In addition, the MDA signal has desirable spectral characteristics. After extracting the reference signal, a low complexity correlation receiver is constructed to demodulate information bits. Detection performance is usually dependent on estimation. But the estimation performance is related to detection in the proposed receiver because the reference estimation is a two-step operation and final estimation depends on initial detection. Therefore, analysis becomes involved. Unlike [8], we do not assume initial estimation is perfect in this paper and obtain accurate analytical results in a closed form. We also compare the proposed estimator with the maximum likelihood (ML) estimator and build their connections.

## II. SYSTEM MODELLING

### A. Signal Model

In an MDA-UWB system, any two neighboring pulses are modulated by different modulation methods, both PPM and PAM. The transmitted signal is given by

$$s(t) = \sum_{n=-\infty}^{\infty} \sum_{i=0}^{N_f-1} [p(t - nT_s - iT_f - \frac{1 - b_n^{(0)}}{2}\sigma) + b_n^{(1)}p(t - nT_s - iT_f - T_d)]. \quad (1)$$

Here,  $p(t)$  is a monocycle,  $T_f$  is the frame duration and  $T_s = N_f T_f$  is the symbol duration. Each frame contains one doublet. Two information bits  $b_n^{(0)}, b_n^{(1)} \in \{\pm 1\}$  are transmitted during the  $n$ th symbol period. The first bit modulates the first pulse using PPM and  $\sigma$  is the modulation delay. The second pulse delayed by  $T_d$  is modulated by PAM. Each bit is transmitted repeatedly in  $N_f$  frames. In order not to be distracted from the main idea, we only consider the special

This work was supported in part by the U. S. Army Research Laboratory under the Collaborative Technology Alliance Program, Cooperative Agreement DAAD19-01-2-0011. The U. S. Government is authorized to reproduce and distribute reprints for Government purposes notwithstanding any copyright notation thereon.

case of  $N_f = 1$  in this paper. That means each information-carried pulse is only transmitted once and the symbol duration is the same as the frame duration. But discussions can be readily extended to repetitive transmissions.

The transmitted signal is distorted by the transmitter antenna, a multipath channel, the receiver antenna and additive white Gaussian noise (AWGN). To better capture the signal energy, we use a filter matched to the transmitted pulse. If we define a new waveform  $w(t) = p(t) \star h(t) \star p(-t)$ , with  $\star$  denoting convolution and  $h(t)$  capturing effects of transmitter, channel and receiver antenna, then we can obtain the following received signal model

$$r(t) = \sum_{n=-\infty}^{\infty} [w(t - nT_s - \frac{1 - b_n^{(0)}}{2}\sigma) + b_n^{(1)}w(t - nT_s - T_d)] + v(t) \quad (2)$$

where  $v(t)$  is approximately AWGN with double-sided power spectral density  $\sigma_v^2 = N_0/2$ . After sampling every  $T_t$  seconds, we obtain discrete-time samples  $r(i) = r(t)|_{t=iT_t}$  as follows

$$r(i) = \sum_{n=-\infty}^{\infty} [w(i - nN_s - \frac{1 - b_n^{(0)}}{2}L) + b_n^{(1)}w(i - nN_s - N_d)] + v(i) \quad (3)$$

where  $N_s, N_d, L$  are integers satisfying  $T_s = N_s T_t$ ,  $T_d = N_d T_t$  and  $\sigma = L T_t$ .  $v(i)$  is the sampled noise. Suppose the duration of  $w(t)$  is  $T_w$  and  $q = \lceil \frac{T_w}{T_t} \rceil$  is the order of the discretized waveform  $w(t)$ .  $T_d$  and  $T_s$  are chosen to be greater than  $T_w + \sigma$  and  $2T_w + \sigma$  respectively to avoid inter-pulse interference as well as inter-symbol interference. We collect first  $q$  samples within the first half frame into vector  $\mathbf{r}_{n,1}$  and similarly put first  $q$  samples within the second half frame into vector  $\mathbf{r}_{n,2}$

$$\mathbf{r}_{n,1} = \mathbf{w} + a_n(\mathbf{J} - \mathbf{I})\mathbf{w} + \mathbf{v}_{n,1}, \quad \mathbf{r}_{n,2} = b_n^{(1)}\mathbf{w} + \mathbf{v}_{n,2}, \quad (4)$$

where  $a_n := \delta(b_n^{(0)} + 1)$ ,  $\delta(\cdot)$  is a Kronecker delta function, and  $\mathbf{J}$  is a square matrix after shifting down all elements of an identity matrix  $\mathbf{I}$  by  $L$  rows and  $\mathbf{J}^0 = \mathbf{I}$ .  $\mathbf{w}, \mathbf{v}_{n,1}, \mathbf{v}_{n,2}$  are corresponding vectors with length  $q$ . In (4), the two separate signal vectors corresponding to two bits are modulated by different modulation schemes. Because the two pulses are transmitted through the same channel, they can be used as references for each other in order to detect information symbols. This will become clear when we discuss the receiver design. In addition, the inherent modulation diversity can be exploited to obtain accurate reference signal and thus improve detection performance. As we shall see shortly, the non-zero mean property of PPM signals will be utilized first to construct a preliminary low complexity template estimator. Then the estimator is improved based on coarse estimates of PPM and PAM inputs in order to achieve better detection performance.

## B. Receiver Structure

In this subsection, we introduce a receiver to demodulate both PPM and PAM bits. Because low complexity is a critical

requirement in most UWB applications, our aim is to design a simple yet powerful receiver to achieve good performance-complexity tradeoff.

In the MDA signal model (4), the information about the pulse shape and multipath channel response is included in the vector  $\mathbf{w}$ . We shall use it as a reference waveform to detect information symbols. It has been observed PPM signals have a nonzero mean [10]. Thus a first-order blind estimator is constructed to obtain an estimate of the reference signal  $\mathbf{w}$ . With (4), the mean of vector  $\mathbf{r}_{n,1}$  is

$$\bar{\mathbf{r}}_1 = E\{\mathbf{r}_{n,1}\} = \frac{1}{2}(\mathbf{I} + \mathbf{J})\mathbf{w}. \quad (5)$$

Use  $N$  data vectors  $\mathbf{r}_{n,1}$  to estimate the mean by sample average  $\hat{\mathbf{r}}_1 = \frac{1}{N} \sum_{n=1}^N \mathbf{r}_{n,1}$  and minimize the estimation error  $\|\hat{\mathbf{r}}_1 - \bar{\mathbf{r}}_1\|^2$ . This yields our initial estimator

$$\hat{\mathbf{w}}_0 = 2\mathbf{T}^{-1}\hat{\mathbf{r}}_1, \quad \mathbf{T} = \mathbf{I} + \mathbf{J}. \quad (6)$$

Although this estimator has a simple structure, it may have poor performance as analyzed later. Fortunately, we can improve it greatly as a result of the diversity design in MDA-UWB systems. With the initial template, a correlation-based detector is used to demodulate both the  $N$  PAM bits and the  $N$  PPM bits in the same interval

$$\begin{aligned} \hat{b}_n^{(0)} &= \text{sgn}((\Psi\hat{\mathbf{w}}_0)' \mathbf{r}_{n,1}), \quad \hat{a}_n = \delta(\hat{b}_n^{(0)} + 1). \\ \hat{b}_n^{(1)} &= \text{sgn}(\hat{\mathbf{w}}_0' \mathbf{r}_{n,2}), \quad n = 1, \dots, N. \end{aligned} \quad (7)$$

Here, the template  $\Psi\hat{\mathbf{w}}_0$  for PPM detection resembles the template in conventional PPM-UWB systems [11] where  $\Psi = \mathbf{I} - \mathbf{J}$ . Once both bits are estimated, their waveforms can be recovered from PPM signal  $\mathbf{r}_{n,1}$  and PAM signal  $\mathbf{r}_{n,2}$ , and used to improve our template estimate. From PAM signal,  $\mathbf{w}$  is extracted as  $\hat{b}_n^{(1)} \mathbf{r}_{n,2}$ . To extract  $\mathbf{w}$  from PPM signal, denote  $\bar{\mathbf{y}}_n$  the vector with first  $q$  samples of the  $n$ th frame and  $\underline{\mathbf{y}}_n$  the vector with samples from  $L$  to  $L + q$ . We can see  $\bar{\mathbf{y}}_n \equiv \mathbf{r}_{n,1}$ . Since  $\hat{a}_n$  can be either zero or one, correspondingly yielding waveform  $\mathbf{w}$  or  $\mathbf{J}\mathbf{w}$  according to (4),  $\mathbf{w}$  can be recovered from  $\mathbf{r}_{n,1}$  by  $\bar{\mathbf{y}}_n + \hat{a}_n(\underline{\mathbf{y}}_n - \bar{\mathbf{y}}_n)$ . Therefore, a cleaner reference signal is obtained through a simple average operation

$$\hat{\mathbf{w}}_1 = \frac{1}{2N} \sum_{n=1}^N [\bar{\mathbf{y}}_n + \hat{a}_n(\underline{\mathbf{y}}_n - \bar{\mathbf{y}}_n) + \hat{b}_n^{(1)} \mathbf{r}_{n,2}]. \quad (8)$$

As we will show in the next section this is a much better estimate than  $\hat{\mathbf{w}}_0$ . It will be used to construct correlation templates for symbol detection. The detection process is similar to (7), with  $\hat{\mathbf{w}}_0$  being replaced by the improved waveform  $\hat{\mathbf{w}}_1$

$$\begin{aligned} \hat{b}_n^{(0)} &= \text{sgn}((\Psi\hat{\mathbf{w}}_1)' \mathbf{r}_{n,1}), \\ \hat{b}_n^{(1)} &= \text{sgn}(\hat{\mathbf{w}}_1' \mathbf{r}_{n,2}). \end{aligned} \quad (9)$$

In order to further improve system performance, we may continue to update the estimate of  $\mathbf{w}$  in an adaptive way for  $n > N$  as more data are received [12],[13]

$$\hat{\mathbf{w}}_{n-N+1} = \mu\hat{\mathbf{w}}_{n-N} + \bar{\mathbf{y}}_n + \hat{a}_n(\underline{\mathbf{y}}_n - \bar{\mathbf{y}}_n) + \hat{b}_n^{(1)} \mathbf{r}_{n,2}, \quad (10)$$

and perform symbol detection using this updated  $\hat{\mathbf{w}}$  each time. Here,  $\mu < 1$  is a forgetting factor, which can be set to a constant value or adjusted dynamically to achieve optimal performance.

In this paper, we present a discrete-time model and digital receivers for MDA-UWB systems. Further study on the quantization effect using low resolution high rate analog-to-digital converters (ADCs) can be carried out but beyond the scope of this paper. Interested readers are referred to [4], [3] for detailed discussions on this topic. In addition, if analog implementation is desired in low complexity and low cost applications, the proposed MDA-UWB system can be implemented in analog circuits because of the unique structure of  $\mathbf{T}$  and consequently  $\mathbf{T}^{-1}$  in (6) as a power series of  $\mathbf{J}$ , equivalently multiple delay operations.

### C. Maximum Likelihood Estimator

Performance of correlation receivers highly depend on how well the template is estimated. In this subsection, we first develop an ML template estimator for the MDA system and then compare it with the estimator used in our proposed receiver.

Consider a time interval of  $NT_s$ . The received data vector is  $\mathbf{r} := [\mathbf{r}_1, \mathbf{r}_2, \dots, \mathbf{r}_N]'$  of size  $N_s N \times 1$ . Corresponding noise-free signal conditioned on the  $2N$ -bit data vector  $\mathbf{b}_i = [b_{1,i}^{(0)}, b_{1,i}^{(1)}, \dots, b_{N,i}^{(0)}, b_{N,i}^{(1)}]'$  ( $i = 1, 2, \dots, 2^{2N}$ ) is  $\mathbf{s}_i$ . Assuming equal *a priori* probabilities of the  $2^{2N}$  data vectors, the likelihood function after ignoring constants irrelevant to  $\mathbf{w}$  is given by [14],[15]

$$p_{\mathbf{r}}(\mathbf{r}|\mathbf{w}) = \sum_{i=1}^{2^{2N}} \exp\left(-\frac{1}{2\sigma_v^2} \|\mathbf{r} - \mathbf{s}_i\|^2\right). \quad (11)$$

Our objective is to maximize this likelihood function. Then the parameter  $\hat{\mathbf{w}}_{ML} = \arg \max_{\mathbf{w}} p_{\mathbf{r}}(\mathbf{r}|\mathbf{w})$  is the ML estimator of  $\mathbf{w}$ . It is shown the ML estimator satisfies the following equation [9]

$$\hat{\mathbf{w}}_{ML} = \frac{1}{2N} \sum_{n=1}^N \left\{ \bar{\mathbf{y}}_n + G_1(\underline{\mathbf{y}}_n - \bar{\mathbf{y}}_n) + G_2 \mathbf{r}_{n,2} \right\}, \quad (12)$$

where

$$G_1 := \left[ \exp\left(\frac{2(\bar{\mathbf{y}}'_n - \underline{\mathbf{y}}'_n)\hat{\mathbf{w}}_{ML} - \|\bar{\mathbf{y}}_n\|^2 + \|\underline{\mathbf{y}}_n\|^2}{2\sigma_v^2}\right) + 1 \right]^{-1},$$

$$G_2 := \tanh\left(\frac{\mathbf{r}'_{n,2}\hat{\mathbf{w}}_{ML}}{\sigma_v^2}\right),$$

and  $\tanh(\cdot)$  is the hyperbolic tangent function. Comparing (12) with (8), we can see  $G_1$  and  $G_2$  play similar roles as  $\hat{a}_n$  and  $\hat{b}_n^{(1)}$ , given by (9). Corresponding decision functions are  $G_1(x) = (e^x + 1)^{-1}$ ,  $G_2(x) = \tanh(x)$ ,  $\delta(\text{sgn}(x) + 1)$  and  $\text{sgn}(x)$  respectively. We can observe some similarities from their plots in Fig. 1. However,  $\delta(\text{sgn}(x) + 1)$  and  $\text{sgn}(x)$  are piecewise functions while  $G_1(x)$  and  $G_2(x)$  are continuous functions. Thus,  $G_1$  and  $G_2$  can be interpreted as soft decisions of  $a_n$  and  $b_n^{(1)}$ . If they are replaced by hard decisions  $\hat{a}_n$

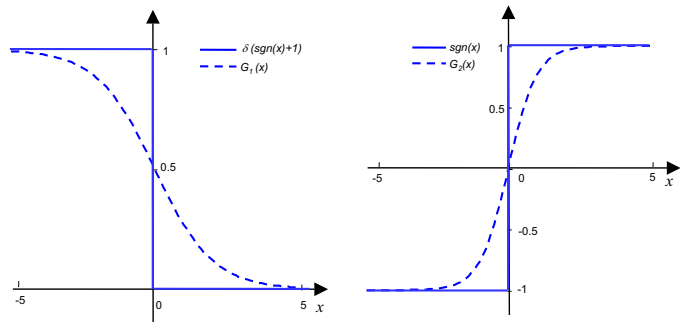


Fig. 1. Illustration of different decision functions.

and  $\hat{b}_n^{(1)}$ , we end up with our proposed estimator (8). It can be expected that the optimal ML estimator  $\hat{\mathbf{w}}_{ML}$  has better performance than the estimator  $\hat{\mathbf{w}}_1$ . But it shows much higher complexity to solve (12) for  $\hat{\mathbf{w}}_{ML}$  because  $G_1$  and  $G_2$  are still highly non-linear functions of  $\hat{\mathbf{w}}_{ML}$ . It has to be solved iteratively. The convergence relies on initialization. If the initial guess is far away from the true vector, the iteration may never converge to the optimum and performance will be very poor. As we will see from simulations, performance degradation of  $\hat{\mathbf{w}}_1$  is marginal compared with  $\hat{\mathbf{w}}_{ML}$ . The good trade-off between performance and complexity motivates our adoption of estimator  $\hat{\mathbf{w}}_1$  instead of  $\hat{\mathbf{w}}_{ML}$ . This suboptimal estimator can even converge to the ML estimator at high signal-to-noise ratio (SNR). To avoid iteration in solving  $\hat{\mathbf{w}}_{ML}$ , one can derive an approximate ML estimator by approximating both nonlinear functions  $G_1$  and  $G_2$  with piecewise linear functions as in [14]. But the solution is found to be unstable with large  $N$ . Due to limited space, we omit detailed discussions here.

### III. PERFORMANCE ANALYSIS

We give performance analysis of the receiver in this section. For correlation receivers, detection performances are dependent on the accuracy of estimated template. Now we first derive the general expression of bit error rate (BER) when a correlation receiver and estimated template  $\hat{\mathbf{w}}$  are used. Then we will evaluate template estimation performance in the measure of mean-square-error (MSE).

Define the template error as  $\delta\mathbf{w} := \hat{\mathbf{w}} - \mathbf{w}$ . Its mean and correlation matrix are  $\mathbf{m} = E\{\delta\mathbf{w}\}$  and  $\mathbf{\Gamma} = E\{\delta\mathbf{w}\delta\mathbf{w}'\}$  respectively. The decision statistic of PPM demodulation in (7) and (9) is

$$D_p = [\Psi(\mathbf{w} + \delta\mathbf{w})]'[\mathbf{w} + a_n(\mathbf{J} - \mathbf{I})\mathbf{w} + \mathbf{v}_{n,1}]. \quad (13)$$

After expansion, it becomes

$$D_p = \mathbf{w}'\Psi'\mathbf{w} - a_n\mathbf{w}'\Psi'\Psi\mathbf{w} + \mathbf{w}'\Psi'\mathbf{v}_{n,1} + \delta\mathbf{w}'\Psi'\mathbf{w} - a_n\delta\mathbf{w}'\Psi'\Psi\mathbf{w} + \delta\mathbf{w}'\Psi'\mathbf{v}_{n,1}. \quad (14)$$

Its mean conditioned on  $a_n = 0$  is

$$E\{D_p|a_n = 0\} = \mathbf{w}'\Psi'\mathbf{w} + \mathbf{m}'\Psi'\mathbf{w}. \quad (15)$$

The variance conditioned on  $a_n = 0$  is

$$\text{Var}\{D_p|a_n = 0\} = \sigma_v^2 \mathbf{w}' \Psi' \Psi \mathbf{w} + \mathbf{w}' \Psi \Pi \Psi' \mathbf{w} + \sigma_v^2 \text{tr}(\Psi \Gamma \Psi') + 2\sigma_v^2 \mathbf{w}' \Psi' \Psi \mathbf{m}, \quad (16)$$

where  $\Pi = \Gamma - \mathbf{m} \mathbf{m}'$  is the covariance matrix of template estimation error. Similarly, the mean and variance conditioned on  $a_n = 1$  are

$$E\{D_p|a_n = 1\} = \mathbf{w}' \Psi' \mathbf{J} \mathbf{w} + \mathbf{m}' \Psi' \mathbf{J} \mathbf{w}, \quad (17)$$

and

$$\text{Var}\{D_p|a_n = 1\} = \sigma_v^2 \mathbf{w}' \Psi' \Psi \mathbf{w} + \mathbf{w}' \mathbf{J}' \Psi \Pi \Psi' \mathbf{J} \mathbf{w} + \sigma_v^2 \text{tr}(\Psi \Gamma \Psi') + 2\sigma_v^2 \mathbf{w}' \Psi' \Psi \mathbf{m} \quad (18)$$

respectively. Then the averaged BER for PPM modulated bits is

$$P_e^{PPM} = \frac{1}{2} Q\left(\frac{E\{D_p|a_n = 0\}}{\sqrt{\text{Var}\{D_p|a_n = 0\}}}\right) + \frac{1}{2} Q\left(-\frac{E\{D_p|a_n = 1\}}{\sqrt{\text{Var}\{D_p|a_n = 1\}}}\right), \quad (19)$$

where  $Q(x) = \int_x^\infty \frac{1}{\sqrt{2\pi}} e^{-\frac{x^2}{2}} dx$ .

From (7), the decision statistic of PAM demodulation is

$$D_A = b_n^{(1)} \mathbf{w}' \mathbf{w} + \mathbf{w}' \mathbf{v}_{n,2} + b_n^{(1)} \delta \mathbf{w}' \mathbf{w} + \delta \mathbf{w}' \mathbf{v}_{n,2}. \quad (20)$$

Its mean and variance conditioned on  $b_n^{(1)} = 1$  are found to be

$$E\{D_a|b_n^{(1)} = 1\} = \mathbf{w}' \mathbf{w} + \mathbf{m}' \mathbf{w}, \quad (21)$$

$$\text{Var}(D_a|b_n^{(1)} = 1) = \sigma_v^2 \mathbf{w}' \mathbf{w} + \mathbf{w}' \Pi \mathbf{w} + \sigma_v^2 \text{tr}(\Gamma) + 2\sigma_v^2 \mathbf{m}' \mathbf{w}. \quad (22)$$

It is easy to verify the error probability conditioned on  $b_n^{(1)} = -1$  is the same as that given  $b_n^{(1)} = 1$ . Because the two values are equally probable in data sequence, the average BER of detecting PAM bits is

$$P_e^{PAM} = Q\left(\frac{E\{D_a|b_n^{(1)} = 1\}}{\sqrt{\text{Var}(D_a|b_n^{(1)} = 1)}}\right). \quad (23)$$

It is clear from (19) and (23) that detection performance is related to the template estimation through  $\mathbf{m}$  and  $\Gamma$ . Next, we will derive these quantities for both proposed estimators  $\hat{\mathbf{w}}_0$  and  $\hat{\mathbf{w}}_1$ .

For the estimator (6), we obtain

$$\delta \mathbf{w}_0 := \hat{\mathbf{w}}_0 - \mathbf{w} = 2\mathbf{T}^{-1} \left( \frac{1}{N} \sum_{n=1}^N \mathbf{r}_{n,1} - \bar{\mathbf{r}}_1 \right). \quad (24)$$

$\delta \mathbf{w}_0$  has zero mean  $\mathbf{m}_0 = 0$  and correlation matrix  $\Gamma_0$  equals covariance  $\Pi_0$

$$\Gamma_0 = \Pi_0 = \frac{4}{N^2} \mathbf{T}^{-1} \sum_{n_1, n_2} E\{\delta \mathbf{r}_{n_1,1} \delta \mathbf{r}'_{n_2,1}\} \mathbf{T}'^{-1}, \quad (25)$$

where  $\delta \mathbf{r}_{n,1} := \mathbf{r}_{n,1} - \bar{\mathbf{r}}_1$ . Under our assumption of no inter-symbol interference,  $\mathbf{r}_{n_1,1}$  and  $\mathbf{r}_{n_2,1}$  are independent for  $n_1 \neq n_2$ . Then (25) can be simplified to

$$\Gamma_0 = \Pi_0 = \frac{4}{N} \mathbf{T}^{-1} E\{\delta \mathbf{r}_{n,1} \delta \mathbf{r}'_{n,1}\} \mathbf{T}'^{-1}. \quad (26)$$

Invoking (4) and (5),  $E\{\delta \mathbf{r}_{n,1} \delta \mathbf{r}'_{n,1}\}$  can be evaluated

$$E\{\delta \mathbf{r}_{n,1} \delta \mathbf{r}'_{n,1}\} = \frac{1}{4} \Psi \mathbf{w} \mathbf{w}' \Psi' + \sigma_v^2 \mathbf{I}. \quad (27)$$

Substituting (27) into (26), we obtain

$$\Gamma_0 = \Pi_0 = \frac{1}{N} \mathbf{T}^{-1} \Psi \mathbf{w} \mathbf{w}' \Psi' \mathbf{T}'^{-1} + \frac{4\sigma_v^2}{N} \mathbf{T}^{-1} \mathbf{T}'^{-1}. \quad (28)$$

The MSE of the estimator  $\hat{\mathbf{w}}_0$  is calculated as the trace of the above matrix. Let us denote the error probabilities of  $\hat{b}_n^{(0)}$  and  $\hat{b}_n^{(1)}$  in (7) as  $P_{0,p}$  and  $P_{0,a}$  respectively. Subscript ‘‘0’’ refers to  $\hat{\mathbf{w}}_0$ , ‘‘p’’ represents PPM and ‘‘a’’ PAM. Then BERs  $P_{0,p}$  and  $P_{0,a}$  are calculated by (19) and (23) after considering  $\mathbf{m} = 0$  and (28).

The analysis of the estimator (8) and corresponding BERs are more complicated because it depends on the detection performance of  $b_n^{(0)}$  and  $b_n^{(1)}$ , and in turn on performance of  $\hat{\mathbf{w}}_0$ . Without loss of generality, we assume all errors appear in the leading positions of any given data block of size  $2N$  bits. The average number of errors among the  $N$  bits for PPM is  $NP_{0,p}$  and that for PAM is  $NP_{0,a}$ . Because wrong detections imply  $\hat{a}_n$  becomes  $1 - a_n$  and  $\hat{b}_n^{(1)}$  becomes  $-b_n^{(1)}$ , the template estimation error  $\delta \mathbf{w}_1 := \hat{\mathbf{w}}_1 - \mathbf{w}$  can be calculated using (8) as

$$\delta \mathbf{w}_1 = \frac{1}{2N} \left\{ \sum_{n=1}^{NP_{0,p}} \left[ \bar{\mathbf{y}}_n + (\mathbf{y}_n - \bar{\mathbf{y}}_n)(1 - a_n) \right] + \sum_{n=NP_{0,p}+1}^N \left[ \bar{\mathbf{y}}_n + (\mathbf{y}_n - \bar{\mathbf{y}}_n)a_n \right] + \sum_{n=1}^{NP_{0,a}} (-b_n^{(1)}) \mathbf{r}_{n,2} + \sum_{n=NP_{0,a}+1}^N b_n^{(1)} \mathbf{r}_{n,2} \right\} - \mathbf{w}. \quad (29)$$

Invoking

$$\bar{\mathbf{y}}_n = \mathbf{w} + a_n (\mathbf{J} \mathbf{w} - \mathbf{w}) + \mathbf{v}_{n,1},$$

$$\mathbf{y}_n = \mathbf{J}' \mathbf{w} + a_n (\mathbf{w} - \mathbf{J}' \mathbf{w}) + \mathbf{J}' \mathbf{v}_{n,1} + \tilde{\mathbf{v}}_{n,1},$$

we obtain

$$\delta \mathbf{w}_1 = \frac{1}{2N} \left\{ \sum_{n=1}^{NP_{0,p}} [\mathbf{J}' \mathbf{w} + a_n (\mathbf{J} \mathbf{w} - \mathbf{J}' \mathbf{w}) - \mathbf{w} + \mathbf{J}' \mathbf{v}_{n,1} + a_n (\mathbf{v}_{n,1} - \mathbf{J}' \mathbf{v}_{n,1}) + (1 - a_n) \tilde{\mathbf{v}}_{n,1}] + \sum_{n=NP_{0,p}+1}^N [\mathbf{v}_{n,1} + a_n (\mathbf{J}' \mathbf{v}_{n,1} - \mathbf{v}_{n,1}) + a_n \tilde{\mathbf{v}}_{n,1}] - 2NP_{0,a} \mathbf{w} - \sum_{n=1}^{NP_{0,a}} b_n^{(1)} \mathbf{v}_{n,2} + \sum_{n=NP_{0,a}+1}^N b_n^{(1)} \mathbf{v}_{n,2} \right\}, \quad (30)$$

where  $\tilde{\mathbf{v}}_{n,1}$  represents a  $q \times 1$  vector with only  $L$  nonzero noise samples appearing at the tail. The mean and covariance matrix of  $\delta \mathbf{w}_1$  can be computed

$$\mathbf{m}_1 = \frac{1}{2} P_{0,p} \left( \frac{1}{2} \mathbf{J}' \mathbf{w} - \mathbf{w} + \frac{1}{2} \mathbf{J} \mathbf{w} \right) - P_{0,a} \mathbf{w}, \quad (31)$$

$$\begin{aligned}
\mathbf{\Pi}_1 &= E\{(\delta\mathbf{w}_1 - \mathbf{m}_1)(\delta\mathbf{w}_1 - \mathbf{m}_1)'\} \\
&= \frac{1}{16N}[(\mathbf{J} - \mathbf{J}')\mathbf{w}\mathbf{w}'(\mathbf{J} - \mathbf{J}')'P_{0,p} \\
&\quad + 6\sigma_v^2\mathbf{I} + 2\sigma_v^2\mathbf{J}'\mathbf{J} + 2\sigma_v^2\tilde{\mathbf{I}}], \quad (32)
\end{aligned}$$

where  $\tilde{\mathbf{I}}$  is a matrix of all zero entries but with only  $L$  ones appearing on the trailing main diagonal. The correlation matrix becomes  $\mathbf{\Gamma}_1 = \mathbf{\Pi}_1 + \mathbf{m}_1\mathbf{m}_1'$ . Substituting  $\mathbf{\Gamma}_1$ , (31) and (32) into (15)-(18), and the corresponding results into (19), we can obtain the BER for PPM bits, denoted as  $P_{1,p}$ . Similarly, using  $\mathbf{\Gamma}_1$ , (31), (32), and (21)-(23), we obtain the BER for PAM bits, denoted as  $P_{1,a}$ .

With the above analytical results, we can gain more insights about performance of estimators  $\hat{\mathbf{w}}_0$ ,  $\hat{\mathbf{w}}_1$  and corresponding receivers. Obviously, the mean of  $\hat{\mathbf{w}}_1$  (31) is nonzero in general. Therefore,  $\hat{\mathbf{w}}_1$  is a biased estimator. But with increasing SNR, both  $P_{0,p}$  and  $P_{0,a}$  decrease and the bias reduces. Despite the bias, the MSE of  $\hat{\mathbf{w}}_1$  is usually much smaller than that of  $\hat{\mathbf{w}}_0$ . To see this point, we notice both  $P_{0,p}$  and  $P_{0,a}$  are below  $10^{-2}$  for medium to high values of SNR. Consequently, applying (31) and (32), it is reasonable to approximate the MSE of  $\hat{\mathbf{w}}_1$ , which is the trace of  $\mathbf{\Gamma}_1$ , with

$$\text{tr}(\mathbf{\Gamma}_1) \approx \text{tr}\left(\frac{1}{16N}[6\sigma_v^2\mathbf{I} + 2\sigma_v^2\mathbf{J}'\mathbf{J} + 2\sigma_v^2\tilde{\mathbf{I}}]\right) = \frac{\sigma_v^2}{2N}q. \quad (33)$$

On the other hand, the trace of the second term of (28) is

$$\begin{aligned}
\text{tr}\left(\frac{4\sigma_v^2}{N}\mathbf{T}^{-1}\mathbf{T}'^{-1}\right) &= \frac{4\sigma_v^2}{N}[q + (q - L) + \dots + (q - dL)] \\
&> \frac{4\sigma_v^2}{N}q, \quad (34)
\end{aligned}$$

where  $d := \lfloor \frac{q}{L} \rfloor$  and we have used the fact that

$$\mathbf{T}^{-1} = \mathbf{I} - \mathbf{J} + \mathbf{J}^2 - \mathbf{J}^3 + \dots$$

As a consequence,  $\text{tr}(\mathbf{\Gamma}_1) < \frac{4\sigma_v^2}{N}q < \text{tr}(\mathbf{\Gamma}_0)$  even if we ignore the first positive term in (28). For low SNR, the above reasoning still holds if  $N$  is not too large because the last three terms of  $\mathbf{\Pi}_1$  dominate in  $\mathbf{\Gamma}_1$ . Thus, we conclude the estimator  $\hat{\mathbf{w}}_1$  improves the performance of  $\hat{\mathbf{w}}_0$  substantially, and much lower probability of error can be achieved if  $\hat{\mathbf{w}}_1$  is used as a correlation template.

#### IV. SIMULATIONS

The transmitted monocycle is chosen as normalized second derivative of Gaussian pulse with effective duration of 0.7ns. A discrete-time IEEE 802.15 multipath channel model CM1 [16] with sampling period 0.1ns is adopted, which describes line-of-sight (LOS) channels between 0 and 4 meters. The tail of channel is truncated so that the maximum delay spread is 40ns. 50 randomly generated channels are used for simulations and are assumed to be static. The receiver is sampled every  $T_t = 0.1$ ns. Other system parameters are chosen as  $T_d = 42$ ns,  $T_s = 84$ ns and PPM modulation delay  $\sigma = 0.8$ ns. SNR is set at  $E_b/N_0 = 15$ dB and the length of data bits employed for template estimation is only  $N = 100$ .

Averaged MSEs of the two template estimators ( $\hat{\mathbf{w}}_0$  and  $\hat{\mathbf{w}}_1$ ) with respect to data length  $N$  are plotted in Fig. 2.

The circle symbol represents the simulated performance of the initial estimator  $\hat{\mathbf{w}}_0$  while star the final estimator  $\hat{\mathbf{w}}_1$ . MSEs decrease with increase of  $N$  for both estimators. The plot confirms our previous conclusion that estimator  $\hat{\mathbf{w}}_1$  significantly outperforms  $\hat{\mathbf{w}}_0$ . The improvement is almost two orders. For verification purpose, we plot the analytical results in the same figure. Analytical curves for both estimators match with corresponding simulations perfectly well. MSE with respect to SNR is presented in Fig. 3. We can still observe linear decreasing of MSE with increase of SNR in this figure. But from analytical expressions (28) and (32), we know there is an error floor above a certain SNR with finite  $N$ . Since this critical SNR is very high, the error floor does not appear within our observation window. ML estimation results are also presented in this figure. It is initialized using our estimator  $\hat{\mathbf{w}}_0$  and obtained after five iterations. We notice the difference between the estimator  $\hat{\mathbf{w}}_1$  and the ML estimator is marginal. The MSE curve of  $\hat{\mathbf{w}}_1$  converges to that of the ML estimator at high SNR. This implies that  $\hat{\mathbf{w}}_1$  is asymptotically optimal.

Next, we examine the error performance of our proposed receivers in Fig. 4. Since performances of PPM bits and PAM bits are different, we plot their BERs separately. A good agreement between analysis and simulations can be observed. Compared with each corresponding ML receiver, the proposed receiver has some performance loss. But the difference diminishes with increase of SNR.

#### V. CONCLUSIONS

Because low complexity and low cost are critical requirements in most UWB systems, a modulation diversity assisted UWB system is particularly suitable for UWB applications. A near-optimum MDA-UWB receiver is studied in this paper. Both estimation performance and detection performance are analyzed in detail. It is shown the proposed receiver employs hard decision functions in reference estimation while a maximum likelihood estimator uses soft-decisions. As a result, the proposed receiver has much lower complexity but is still able to attain the same performance as ML receivers at high SNR.

#### REFERENCES

- [1] R. T. Hoctor and H. W. Tomlinson, "Delay-hopped transmitted reference RF communications," in *Proc. 2002 UWBST*, Baltimore, MD, May 2002, pp. 265–270.
- [2] J. D. Choi and W. E. Stark, "Performance of ultra-wideband communications with suboptimal receivers in multipath channels," *IEEE J. Selected Areas Commun.*, vol. 20, no. 9, pp. 1754–1766, Dec. 2002.
- [3] J. Tang, Z. Xu, and B. M. Sadler, "Performance analysis of b-bit digital receivers for TR-UWB systems with inter-pulse interference," *IEEE Trans. Wireless Communications*, (submitted).
- [4] —, "Digital receiver for TR-UWB systems with inter-pulse interference," in *Proc. of IEEE SPAWC*, New York, June 2005.
- [5] J. Romme and K. Witrisal, "Analysis of QPSK transmitted-reference systems," in *Proc. of IEEE Intl. Conf. on Ultra-Wideband*, Sept. 2005, pp. 502–507.
- [6] T. Zasowski, F. Althaus, and A. Wittneben, "An energy efficient transmitted-reference scheme for ultra wideband communications," in *Proc. of 2004 UWBST*, Kyoto, Japan, May 2004.
- [7] L. Yang and G. B. Giannakis, "Optimal pilot waveform assisted modulation for ultra wideband communications," *IEEE Trans. Wireless Commun.*, vol. 3, no. 4, pp. 1236–1249, July 2004.

- [8] J. Tang and Z. Xu, "A novel modulation diversity assisted ultra wideband communication system," in *Proc. of ICASSP'05*, Philadelphia, PA, March 2005.
- [9] —, "A novel modulation diversity assisted ultra-wideband communication system," *IEEE Trans. Signal Processing*, (submitted).
- [10] Z. Xu, J. Tang, and P. Liu, "Multiuser channel estimation for ultra-wideband systems using up to the second order statistics," *EURASIP Journal on Applied Signal Processing: Special Issue on UWB - State of the Art*, vol. 2005, no. 3, pp. 273–286, Mar. 2005.
- [11] M. Z. Win and R. A. Scholtz, "Ultra-wide bandwidth time-hopping spread-spectrum impulse radio for wireless multiple-access communications," *IEEE Trans. Commun.*, vol. 48, no. 4, pp. 679–689, Apr. 2000.
- [12] Z. Xu, "Trends in ultra-wideband transceiver design," Chapter 7 in *Ultra-Wideband Wireless Communications and Networks*, S. Shen, M. Guizani, R. C. Qiu, and T. Le-Ngoc (editors), Hoboken, NJ: John Wiley & Sons, 2006.
- [13] S. Zhao, H. Liu, and Z. Tian, "Decision directed autocorrelation receivers for pulsed ultra-wideband systems," *IEEE Trans. on Wireless Comm.*, vol. 5, no. 8, August 2006.
- [14] S. Franz and U. Mitra, "On optimal data detection for UWB transmitted reference systems," in *Proc. IEEE Globecom*, vol. 2, San Francisco, CA, Dec. 2003, pp. 744–748.
- [15] —, "Generalized UWB transmitted reference systems," *IEEE J. Selected Areas in Commun.*, vol. 24, no. 4, pp. 780–786, April 2006.
- [16] IEEE P802.15 Working Group, "Channel modeling sub-committee report final," IEEE P802.15-02/490r1-SG3a, Feb. 2003.

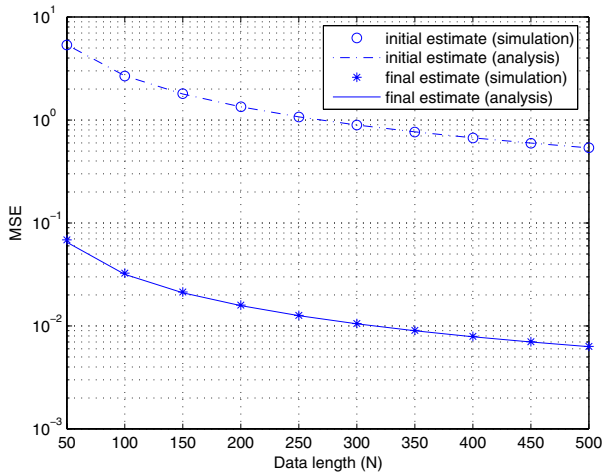


Fig. 2. MSE of two template estimators under  $E_b/N_0=15\text{dB}$ .

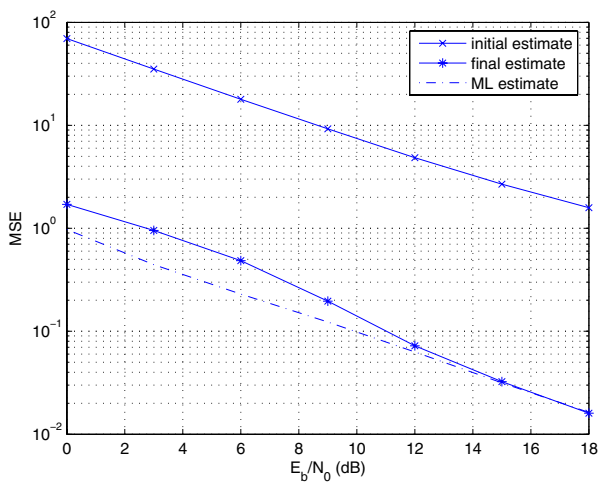


Fig. 3. Effect of SNR on estimation performance with  $N = 100$ .

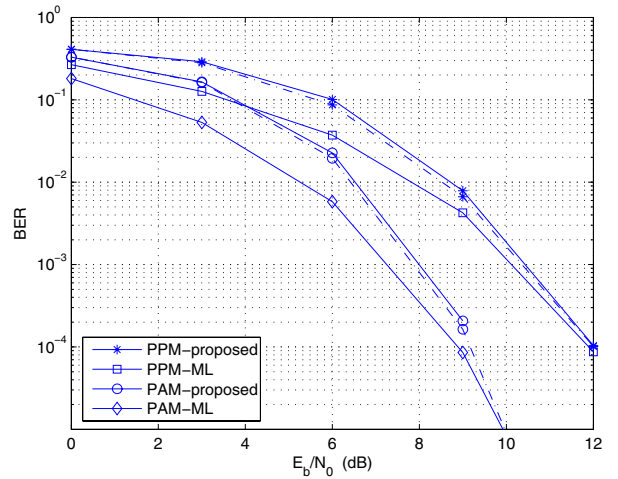


Fig. 4. Comparison of MDA and ML receivers. Solid lines: simulation results; dash-dotted lines: analytical results.